

# ESTIMATING EARTHQUAKE AND LANDSLIDE TSUNAMI HAZARD FOR THE NEW ZEALAND COAST

W.P. de Lange<sup>1</sup> and V.G. Moon<sup>1</sup>

## ABSTRACT

Tsunamis are a significant hazard on the New Zealand coast, with historic events being mostly generated by submarine earthquakes and landslides. Historical data combined with numerical modelling provides the best estimates of potential tsunami behaviour, but requires more data than is normally available for New Zealand. Simple parametric models provide useful estimates of maximum tsunami amplitude for seismic and landslide generation mechanisms, and a viable approach to characterise potential tsunami hazard.

## 1.0 INTRODUCTION

New Zealand experiences a similar frequency of tsunamis with amplitudes >1 m as Hawaii and Indonesia, and about a third of that experienced in Japan (de Lange, 2000). This represents a significant hazard, particularly to low-lying coastal regions surrounding estuaries. The types of hazards involved were highlighted in this Bulletin by the New Zealand Reconnaissance Team report into the 17<sup>th</sup> July 1998 tsunami in Papua New Guinea (Goldsmith et al., 1999).

In terms of hazard, tsunamis affecting New Zealand may be loosely grouped into those generated beyond the continental margins (*distant tsunamis*), and those generated on or within the continental margins (*local tsunamis*). Since AD 1800 distant tsunamis have typically reached maximum amplitudes of 1-3 m along the New Zealand coast, although some locations, such as Banks Peninsula experience larger waves due to local amplification. Areas susceptible to amplification of distant tsunami can be identified from historic data (de Lange and Healy, 1986), and the application of numerical models (Walters, 2002).

Distantly generated tsunami waves have propagation times exceeding 2 hours for known tsunami sources in the Pacific Ocean. This is sufficient time for the Pacific Tsunami Warning Centre to evaluate the tsunami characteristics and initiate a response in New Zealand. Therefore, the hazard represented by distant tsunami is relatively straightforward to characterise using historic data, and mitigation is also manageable.

Locally generated tsunami waves arrive at the shore less than 2 hours after generation, in many cases within minutes. This makes mitigation after generation very difficult, and a proactive approach is required. In order to design a mitigation strategy that is effective, it is useful to have an indication of the likely tsunami amplitude. The tsunami amplitude is initially a function of the source magnitude and mechanism of tsunami generation.

Historic and palaeotsunami data indicate that there are three main source events for locally generated tsunamis: earthquakes, landslides and volcanic eruptions. Although

volcanic eruptions may have generated the largest tsunami in New Zealand over the last few millennia, these events are rare and poorly understood. The majority of local tsunami events have been associated with earthquakes, and a small number are due to landslides (de Lange and Healy, 1986). The landslide events are of concern as they include the largest historic tsunami events, and they do not necessarily involve an earthquake, so therefore there is little warning before they arrive. This paper outlines simple procedures for estimating tsunami amplitude for local coseismic and landslide tsunamis.

## 2.0 PREDICTING TSUNAMI AMPLITUDE

Determining the potential tsunami amplitude for any region of the coast requires a reasonably complete understanding of the source mechanism. This allows the application of numerical models to simulate tsunami generation. If suitable bathymetric data are available, the propagation of the tsunami can also be simulated, resulting in detailed predictions of the temporal and spatial tsunami behaviour at the shore. By hindcasting known events, this information can be calibrated and used for hazard mitigation.

Unfortunately the data required to define source mechanisms, simulate tsunami propagation and calibrate the results are often of poor quality or absent for New Zealand. Parametric methods provide an alternative approach with less stringent data requirements that allow estimation of the maximum tsunami hazard.

### 2.1 Coseismic tsunami

There are clear correlations between the magnitude of earthquakes and the magnitude of tsunamis generated by coseismic processes. This allows tsunami amplitude to be estimated from the earthquake magnitude. One method commonly used is the Abe tsunami magnitude scale (Abe, 1979; Abe, 1995), given by

$$M_t = \log_{10} a + B = \log_{10} a + C \log_{10} R + D \quad (1)$$

where  $M_t$  is the tsunami magnitude, defined by  $M_t = \log_{10}(r/r')$  where  $r$  is maximum vertical runup close to source, and  $r'$  is a reference runup of 1 m;

<sup>1</sup> Department of Earth Sciences, University of Waikato, N.Z.

- $a$  is the maximum tsunami amplitude (half the trough to crest distance);
- $R$  is the distance from the earthquake epicentre to tsunami observation site;
- $B, C, D$  are site specific constants.

Normally the constant  $B$  in equation (1) is chosen so that the tsunami magnitude equals the moment magnitude of the generating earthquake ( $M_t = M_w$ ). This allows the tsunami amplitude to be predicted for future earthquakes (Blackford, 1984). Unfortunately, the available tsunami amplitude data for New Zealand are very sparse (de Lange and Healy, 1986), making it very difficult to determine the values of the constant ( $B$ ).

Abe (1995) modified equation (1) based on average constants for a range of large tsunami events in the Pacific, particularly around Japan. Expressing the relationship in terms of the maximum tsunami amplitude, he derived

$$\log_{10} H_{\max} = M_w - \log_{10} R - 5.55 + C \quad (2)$$

where  $H_{\max}$  is the maximum tsunami amplitude (equivalent to height for tsunami);

$M_w$  is the moment magnitude of the generating earthquake;

$R$  is the distance from source (km);

$C$  is a constant reflecting the tectonic setting of the earthquake ( $C=0.0$  for fore-arc settings and  $C=0.2$  for back-arc settings).

This relationship gives unreasonably high amplitudes for small values of  $R$  (Abe, 1995), so equation 2 should only be applied when the distance to source exceeds a minimum value given by

$$\log_{10} R_{\min} = 0.5M_w - 2.25 \quad (3)$$

where  $R_{\min}$  is the minimum distance (km).

Closer to the source than this distance, the maximum tsunami amplitude is given by

$$\log_{10} H_{\max} = 0.5M_w - 3.3 + C \quad (4)$$

There are limited data available for New Zealand to test Equation 4, and these are summarised in Figure 1. The solid and dashed lines represent Equation 4 for back-arc ( $C=0.2$ ) and fore-arc ( $C=0.0$ ) settings respectively. Tsunamis that were clearly coseismic (1855, 1922, 1929, 1931 & 2003) all plot below the back-arc line. The 1950 event is uncertain, and may not represent a tsunami. The remaining events are known to be local tsunamis associated with a landslide (1913 and 1931a), or are probably associated with submarine landslides (March and May 1947). Therefore, it appears that the Abe (1995) method is a suitable predictor of maximum tsunami wave height for historic New Zealand tsunamis, assuming a back-arc tectonic setting ( $C=0.2$ ). Comparisons between numerical simulations of seismic tsunamis generated in the Firth of Thames and the Abe (1995) method also demonstrated that the results were consistent (Chick *et al.*, 2001a; Chick *et al.*, 2001b).

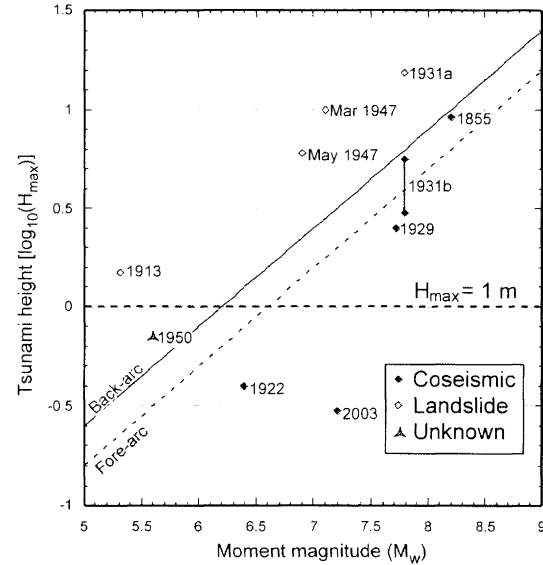


**Figure 1:**  $\log_{10}$  of maximum tsunami wave height versus earthquake moment magnitude for historical local New Zealand tsunami events. The solid and dashed lines represent the predicted maximum height using Equation 4 for back-arc and fore-arc tectonic settings (Abe, 1995). The 1931 Napier earthquake generated two separate tsunamis: (1931a) a very localised 15.3 m high tsunami due to a landslide in the Waikari River estuary; and (1931b) a coseismic tsunami with a maximum height in the range 3-5.5 m (actual height is uncertain due to the coastal uplift associated with this earthquake).

Figure 1 and Equation 4 indicate that the minimum earthquake magnitude required to generate a potentially catastrophic tsunami ( $H_{\max} \geq 1$  m) is around  $M_w = 6.2$ . Equation 4 can also be combined with existing seismic frequency-magnitude distributions for New Zealand (*viz.* Stirling *et al.*, 2002) to estimate the coseismic tsunami hazard. The difficulty is that only some earthquakes generate tsunamis, so it is necessary to estimate the proportion of tsunamigenic events. The data summarised in Figure 1 are inadequate to reliably estimate this proportion.

## 2.2 Tsunami earthquakes

Gusiakov (2001) assessed an alternative relationship between tsunami intensity and earthquake moment magnitude for New Zealand. The tsunami intensity is measured on the Soloviev-Imamura scale defined by (Chubarov and Gusiakov, 1985)

$$I = \frac{1}{2} + \log_2 \bar{H} \quad (5)$$

where  $I$  is the tsunami intensity (Soloviev-Imamura scale);

$\bar{H}$  is the average tsunami inundation height (m) over the length of coast significantly affected by tsunami activity.

The tsunami intensity is related to the earthquake moment magnitude by (Chubarov and Gusiakov, 1985)

$$I = 3.55M_w - 27.1 \quad (6)$$

Gusiakov (2001) applied Equation 6 to 293 Pacific tsunamigenic earthquakes and determined the difference between the observed intensity and the predicted intensity ( $\Delta I$ ). This resulted in three distinct groups of tsunamigenic earthquakes:

*Red earthquakes* ( $\Delta I > 1$ ) – observed tsunami intensities were larger than predicted. These events mostly were located in shallower water (100-1500 m) within marginal seas, or areas of high sedimentation, or on steep continental slopes;

*Green earthquakes* ( $-1 \leq \Delta I \leq 1$ ) – observed tsunami intensities were similar to those predicted. These events were located in mid-continental slope water depths (1500-2000 m);

*Blue earthquakes* ( $\Delta I < -1$ ) – observed tsunami intensities were much less than predicted. These events were located in deep water (2000-4000 m), or areas of very low sedimentation.

Given the same earthquake magnitude, the earthquake source mechanism is often considered to be the major factor controlling tsunami intensity or magnitude (*viz.* Geist, 1998). However, various numerical and physical modelling studies have shown that the largest difference (between strike-slip and reverse dip-slip or low angle thrust mechanisms) is around one order of magnitude for wave height (Hammack, 1973; Ward, 1980). This is insufficient to account for the observed variation, particularly for red earthquakes. Most of these events have also been classified as *tsunami earthquakes* due to a variety of distinguishing seismological characteristics (Kanamori, 1972).

It is recognised that tsunami earthquakes are associated with significant thicknesses of sediment, as are *red earthquakes* (Gusiakov, 2001), and various models involving unusual slip distributions or rupture characteristics, combined with refraction of the resulting tsunami waveforms have been proposed to explain the higher than expected tsunami magnitude (*viz.* Geist and Dmowska, 1999; Goldsmith *et al.*, 1999; Satake and Tanioka, 1999). However, since the 1998 event in Papua New Guinea there has been a growing consensus that submarine landslides may account for the extra tsunami energy (Bardet *et al.*, 2003). Although Gusiakov (2001) considers the New Zealand region (bounded by Australia to the east, Tuvalu to the north, Macquarie Island to the south, and 170°W longitude to the east) as predominantly *green* and *blue earthquakes*, regions of the New Zealand continental shelf are characterised by both *red earthquakes* and high sedimentation. These are the east coast of the North Island from East Cape to Hawke Bay, and the west coast of the South Island between the Buller and Haast Rivers (Gusiakov, 2001; Hicks *et al.*, 2003).

### 2.3 Landslide tsunami

For a tsunami generated by a landslide, the main factors affecting the generated wave characteristics are the landslide dimensions (Figure 2) and flow velocity, the water depths where the landslide starts and comes to rest, and the relative density of the landslide material to that of the receiving water.

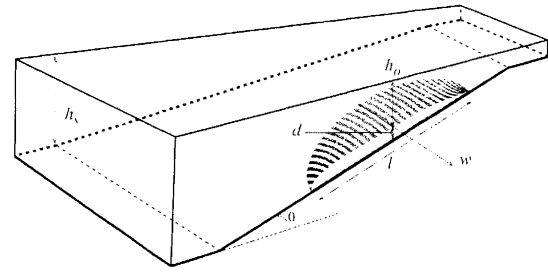


**Figure 2:** Definition of the static parameters that characterise tsunami generation by submarine landslides:  $l$ ,  $w$ , and  $d$  are the landslide length, width and thickness respectively;  $h_0$  and  $h_s$  are the water depths over the initial landslide mid-point and base of the slope; and  $\theta$  is the slope angle.

Pelinovsky and Poplavsky (1997) found that when the length of the landslide is much greater than the water depth over the slide mid-point ( $l \gg h_0$ ), the maximum wave height in the source region is given by

$$H_{\max} = \frac{\pi d^2}{4h_0} \quad (7)$$

where  $d$  is the landslide thickness;

$h_0$  is the water depth over the landslide mid-point.

Hence, the tsunami wave height depends only on the thickness of the landslide and the water depth at source. Following the 1998 tsunami in Papua New Guinea, considerable effort has gone into developing more sophisticated models of tsunami generation by submarine landslides. These studies have found that the key parameters controlling tsunami amplitude are the landslide thickness, the initial water depth, the vertical drop, and the width of the landslide (Ruff, 2003). If the ratio of the initial water depth to the vertical drop is  $> 1$ , then a tsunami is unlikely to be generated. For values  $< 1$ , then the maximum tsunami wave height is approximately equal to the landslide thickness (Ruff, 2003).

Landslide tsunami models have concentrated on two main types of landslide: relatively thin slides ( $d/l \approx 0.5-2\%$ ); and relatively thick slumps ( $d/l \approx 5-15\%$ ). This focus arose due to surveys of the continental margins of the USA that indicated about half of submarine landslides were slides and the rest were slumps (Boon and Berquist, 1991). For a thin slide, the maximum tsunami wave height at source is given by (Watts *et al.*, 2003; McAdoo and Watts, 2004):

$$H_{\max} = 0.224d \left( \frac{l}{h_0} \right)^{1.25} \left( \frac{w}{w + \lambda_0} \right) [\sin^{1.29} \theta - 0.75 \sin^{2.29} \theta + 0.17 \sin^{3.29} \theta] \quad (8)$$

where  $l$  is landslide length;

$w$  is landslide width;

$\theta$  is the slope angle;

$\lambda_0$  is the characteristic tsunami wavelength at source, given by

$$\lambda_0 = 3.87 \sqrt{\frac{l h_0}{\sin \theta}} \quad (9)$$

Equation 8 holds for  $\theta < 30^\circ$ ,  $d/l < 0.2$  and  $h_0/l > 0.06$ . Compared with the full numerical models from which the equation was derived it has an intrinsic accuracy of  $\pm 5.3\%$  (McAdoo and Watts, 2004).

Apart from being thicker, slumps involve a rotational motion and generally do not move the displaced material far from its' initial position. The maximum tsunami wave height at source is given by (Watts *et al.*, 2003; McAdoo and Watts, 2004):

$$H_{\max} = 0.0654d \left( \frac{l}{h_0} \right)^{1.25} \left( \frac{w}{w + \lambda_s} \right) (\sin \theta)^{0.22} \omega^{1.39} \left( \frac{r}{l} \right)^{0.37} \quad (10)$$

where  $\omega$  is the amount of slump rotation in radians;

$r$  is the failure plane radius of curvature.

For a slump, the characteristic tsunami wavelength at source is given by

$$\lambda_s = 1.84 \sqrt{r h_0} \quad (11)$$

Equation 10 holds for  $\theta < 30^\circ$ ,  $d/l < 0.2$ ,  $h_0/l > 0.06$ ,  $\omega < 0.53$  and  $1 < r/l < 2$ , and has an intrinsic accuracy of  $\pm 2.1\%$  (McAdoo and Watts, 2004).

### 3.0 APPLICATION TO NEW ZEALAND TSUNAMIS

#### 3.1 1855 Wairarapa Tsunami

The magnitude 8+ 1855 Wairarapa earthquake generated the largest documented local New Zealand tsunami of the 19<sup>th</sup> Century (Grapes and Downes, 1997). Figure 3 summarises the available data for the observed heights of the tsunami and seismic seiche associated with this event. The Abe Method predicts the maximum tsunami amplitude observed (~9 m at Te Kopi in Palliser Bay). Further, the predictions provide an upper bound for the maximum seismic seiche height, with the exception of the largest value reported for the Wairoa

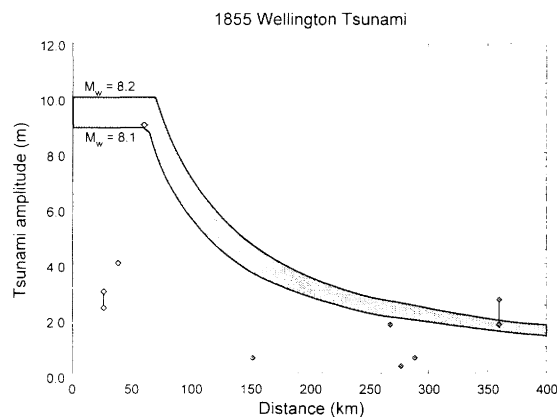


**Figure 3:** Summary of the observed tsunami heights (open diamonds) and seismic seiche heights (filled diamonds) reported by Grapes and Downes (1997) for the 1855 Wairarapa Earthquake with additional data from Downes (pers. comm., 2004). Also plotted is the expected maximum tsunami amplitude predicted by the Abe Method, assuming a moment magnitude in the range 8.1-8.2.

River, Hawke's Bay. As this value was originally documented as "was dashing on the bank two or three yards above its usual height" there is some uncertainty as to the actual height (Grapes and Downes, 1997).

#### 3.2 2003 Fiordland Tsunami

The magnitude of the 2003 Fiordland Earthquake ( $M_w = 7.2$ ) was at the lower limit normally considered as capable of generating a significant tsunami. This event generated a small tsunami that was reported from tide gauges in Jackson Bay and Port Kembla (Table 1), as well as localised larger waves associated with landslides within the fiords (Reyners *et al.*, 2003). The observed tsunami amplitude at Jackson Bay is in good agreement with the maximum amplitude predicted by the Abe Method. However, the amplitude reported from Port Kembla is much larger than predicted and may not represent a tsunami directly generated by this earthquake.

**Table 1:** Summary of observed tsunami amplitudes for the 2003 Fiordland Earthquake (Reyners *et al.*, 2003), and the maximum tsunami amplitude predicted by the Abe Method.

Location	Observed tsunami amplitude (m)	Distance from epicentre (km)	Predicted maximum tsunami amplitude (m)
Jackson Bay	0.30	190	0.37
Port Kembla, New South Wales	0.15	1805	0.04

#### 3.3 1947 Tsunamis

The March and May 1947 tsunamis (Figure 1) are unusual in a number of respects: Firstly, there was a significant discrepancy between the local ( $M_L$ ) and surface wave ( $M_S$ ) magnitudes of the associated earthquakes. This led to their identification as "slow" or "tsunami" earthquakes (Eiby, 1982a). Secondly, the tsunami exhibited a number of unusual characteristics: the wave heights were larger than expected for the magnitude of the earthquakes; the waves appear to have been aperiodic and few in number, with successive waves arriving before the complete withdrawal of the preceding waves; and the wave height distribution was highly focussed, with a faster decay with distance and bearing from the epicentre than would be expected for a coseismic tsunami (Figure 4).

The Abe (1995) model does not consider the effects of bathymetry on the propagating wave: wave height may increase due to resonance and focussing due to wave refraction; or decrease due to wave refraction, diffraction, reflection and dissipation. The amount of amplification that occurs is site specific and depends on the characteristics of the shoaling tsunami (particularly period and approach direction), and the local bathymetry. Resonance has been evaluated at regional scales around the New Zealand coast by Walters (2002).

For the March 1947 tsunami data, the deviations from the predicted wave height are too large and affect too much coast to be attributed to amplification during propagation as has

been demonstrated by numerical modelling (de Lange and Healy, 1997; Magill, 2001). Propagation across the shelf from the inferred source regions for coseismic tsunami results in significant attenuation requiring an initial source amplitude of  $>10$  m. Magill (2001) considered a range of landslide source dimensions and locations for the generation of the March 1947 tsunami, and found that a slide with a thickness of 125 m, total length of 6000 m and source area of  $9 \text{ km}^2$  located at top of the continental slope best replicated the observed tsunami characteristics.

Side-scan, multi-beam and sub-bottom profile data indicate that landslides with volumes ranging from  $10^0$ - $10^4 \text{ km}^3$  are ubiquitous features of the continental margin (Lewis *et al.*, 2001; Lamarche *et al.*, 2002), including in the source region for the 1947 tsunamis proposed by Magill (2001). Although data are not available for the slides or slumps that may have generated the 1947 tsunamis, slides further south typically occur in water depths of 250-500 m, with slope angles of  $1$ - $1.5^\circ$ , thicknesses of 20-70 m, and lengths of 400-4000 m. Slumps occur in water depths of 600-900 m, with slope angles of  $5^\circ$  and thicknesses of 70-140 m (Barnes and Lewis, 1991). Figure 5 shows the source amplitudes for landslide-generated tsunami for a range of mid-slide water depths and

landslide thicknesses predicted by Equation 7. The shaded area corresponds to the landslide characteristics listed above. The depths are consistent with the epicentre location for the March 1947 tsunami (Downes *et al.*, 2001b), and the landslide characteristics are consistent with the numerical modelling results of Magill (2001).

Applying Equation 8 to the slide characteristics discussed above, the predicted maximum source tsunami amplitude ranges over 0.1-4.5 m, which is consistent with the lower-left corner of Figure 5, and are less than the source amplitudes required to account for the March 1947 tsunami (10-20 m). Equation 10 is harder to apply as the amount of slump rotation and failure plane radius of curvature is difficult to determine from the data of Barnes and Lewis (1991). Substituting the full range of possible values for  $\omega$  and  $r$  in combination with the characteristics discussed above, predicts source amplitudes of 0.7-50 m. The critical parameter is  $\omega$ , where a change from 0.1 to 0.5 radians causes an order of magnitude change in tsunami amplitude. It is evident that a slump would account for the observed March 1947 tsunami, as predicted by Magill (2001).

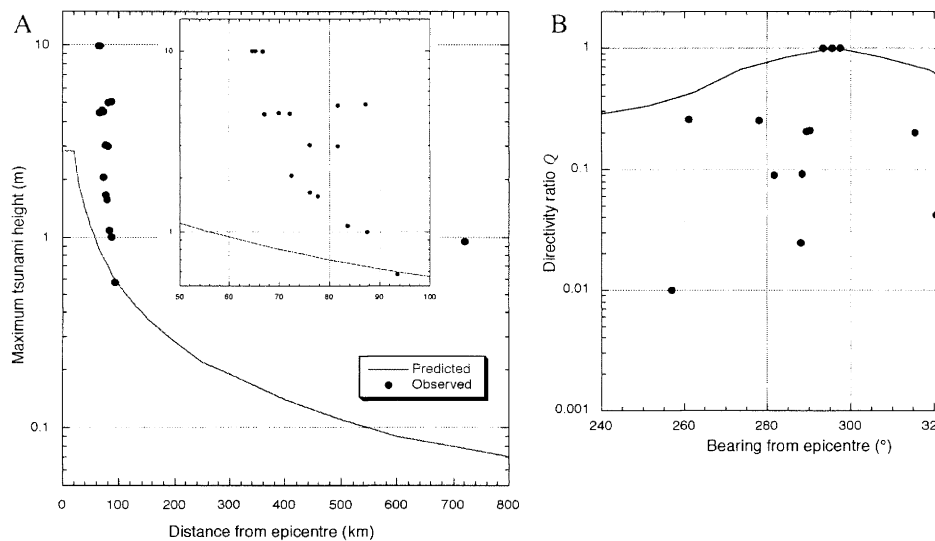


**Figure 4:** Comparisons between observed tsunami characteristics as reported by Downes *et al* (2001a) for the March 1947 earthquake and predicted responses: (A) maximum wave height versus distance from source using the Abe (1995) method (Equations 2-4); and (B) directivity ratio  $Q$  (ratio of tsunami energy at a specific bearing to maximum energy) versus the bearing from the epicentre predicted by Iwasaki (1997). The inset in A highlights the wave heights from the 115 km section of coast between Mahia and Tokomaru Bay. The observed wave heights are larger, and decay faster with distance than is predicted for a coseismic tsunami. Similarly the observed  $Q$  decays faster than predicted for a coseismic tsunami. The observed wave height at  $\sim 720$  km from source plotted in A is not reliable (Downes, pers. comm., 2003).

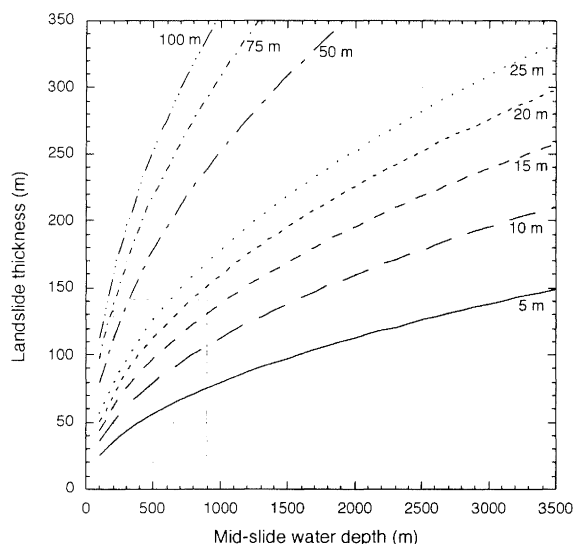


**Figure 5:** *Landslide thicknesses producing specified tsunami heights at source as predicted by Equation 7. The water depths represent outer continental shelf to lower continental slope source regions. The shaded region corresponds to measured landslide thicknesses and source depths for small to medium landslides along the eastern continental margin of New Zealand (Barnes and Lewis, 1991).*

Further, the range of amplitudes predicted by Equation 10 for slump generated tsunamis are the same as those in Figure 5, suggesting that in the absence of data on landslide characteristics, Equation 7 and Figure 5 provide a useful estimate of maximum tsunami amplitudes for landslide tsunami.

### 3.4 Assessing tsunami hazard

The equations discussed above can be used to assess future tsunami hazard, and this is illustrated for Tolaga Bay, located 60 km northeast of Gisborne on the east coast of the North Island of New Zealand. It is the home of the longest wharf in New Zealand (660 m) and possibly the southern hemisphere. It is subject to storm waves up to 3.5 m in height, and during the 20<sup>th</sup> Century has experienced 3 locally generated tsunami:

- While the wharf was under construction in 1927, during calm weather 3 very large waves (6-7 m) caused damage to piles and the pile driver (White-Parsons, 1944). No local earthquake was recorded and the maximum amplitude is unknown.
- 26 March 1947, a few waves reaching 2 m above high tide associated with a  $M_w=6.0$  earthquake. The maximum tsunami amplitude at the coast exceeded 10 m (Eiby, 1982b; Downes *et al.*, 2001b).
- 17 March 1947, unknown number of waves reaching 6 m above high tide associated with a  $M_w=5.6$  earthquake. The maximum tsunami amplitude at the coast exceeded 6 m (Eiby, 1982b; Downes *et al.*, 2001b).

Offshore from Tolaga Bay, the continental shelf is relatively narrow (30-35 km) and drops into the Hikurangi Trench with average depths of 3000-3500 m at 60 km from the coast.

Tolaga Bay lies within the fold and thrust belt of the Hikurangi subduction zone and has experienced up to 27 m of uplift during the Holocene (Berryman *et al.*, 1989). Offshore from Tolaga Bay lie major faults associated with the subduction interface (Stirling *et al.*, 2002). Based on paleoseismic data and probabilistic seismic hazard analysis, coastal uplift is associated with earthquake magnitudes of  $M_w=7.3-8.0$  (Berryman *et al.*, 1989), and recurrence intervals are 600-640 yr for  $M_w=7.7$  and 1230-1300 yr for  $M_w=8.1$  (Stirling *et al.*, 2002). Applying Equation 4, a  $M_w=7.7$  earthquake corresponds to a maximum near-source amplitude of 5.6 m and  $M_w=8.1$  to 8.9 m. Assuming every earthquake of these magnitudes generates a tsunami, the recurrence intervals are ~620 and ~1265 years respectively. Further, a potentially catastrophic tsunami ( $H_{max} \approx 1$  m) requires a minimum earthquake magnitude of  $M_w=6.2$ .

An assessment of subaerial landslides in New Zealand suggests that the minimum earthquake magnitude required to induce subaerial landslides is  $M_w=4.6-5$ , with significant landsliding occurring for  $M_w>6$  (Hancox *et al.*, 2002). Taking a minimum magnitude of  $M_w=5$ , there were 7 earthquakes capable of generating submarine landslides offshore from Tolaga Bay occurred between 1901 and 1993 (Dowrick and Rhoades, 1998), two of which were associated with large tsunami. During this period, a further large tsunami occurred that did not correspond with known earthquakes. It is likely that the recurrence interval for large landslide-generated tsunami is 13-45 years; considerably less than that for catastrophic coseismic tsunami (> 600 yr). The available landslide data for New Zealand indicate that the larger, and more importantly thicker, landslides are associated with the larger, less frequent earthquakes (Hancox *et al.*, 2002; Reyners *et al.*, 2003). The necessary data to quantify this for submarine landslides are not available. However, it seems reasonable to assume that smaller landslides are more frequent than larger events, and therefore the landslide tsunami height at source is more likely to be 5-15 m than 20-50 m (Equation 7 and Figure 5).

### 4.0 CONCLUSIONS

The Abe (1995) method for a back-arc setting (Equations 2-4) provides a conservative estimate of the maximum tsunami amplitude resulting from a seismic source that is consistent with historic New Zealand tsunamis and numerical simulations of potential tsunamis. The method can be combined with magnitude-frequency data for earthquakes to provide estimates of the maximum tsunami amplitude for the New Zealand coast.

Similarly, the Pelinovsky and Poplavsky (1997) method (Equation 7) provides reasonable estimates of the maximum tsunami amplitude resulting from submarine landslides. More complicated methods are available (Equations 8-11) that provide a more reliable estimate if sufficient data exist to characterise the source landslides. These methods can be used to estimate the tsunami amplitude for a range of scenarios. However, at present insufficient data exist to derive frequency-magnitude relationships for submarine landslides comparable to those for earthquakes.

The relationships presented in this paper can be used to provide a conservative estimate of the maximum tsunami amplitude resulting from seismic and landslide sources. This can be used to assess the likely tsunami hazard, and determine whether more expensive numerical simulations are warranted.

## 5.0 REFERENCES

- Abe, K., (1979). "Size of great earthquakes of 1837-1974 inferred from tsunami data". *Journal of Geophysical Research*, **84**, 1561-1568.
- Abe, K., (1995). "Estimate of tsunami run-up heights from earthquake magnitudes". In: Tsuchiya, Y., Shuto, N., (eds.), *Tsunami: Progress in prediction, disaster prevention and warning*, Dordrecht: Kluwer Academic Publishers. pp. 21-35.
- Bardet, J.P.; Synolakis, C.E.; Davies, H.L.; Imamura, F., Okal, E.A., (2003). "Landslide tsunamis: Recent findings and research directions". *Pure and Applied Geophysics*, **160**, 1793-1809.
- Barnes, P.M., Lewis, K.B., (1991). "Sheet slides and rotational failures on a convergent margin: the Kidnappers Slide, New Zealand". *Sedimentology*, **38**, 205-221.
- Berryman, K.R.; Ota, Y., Hull, A.G., (1989). "Holocene paleoseismicity in the fold and thrust belt of the Hikurangi subduction zone, eastern North Island, New Zealand". *Tectonophysics*, **163**, 185-195.
- Blackford, M.E., (1984). "Use of the Abe magnitude scale by the tsunami warning system". *Science of Tsunami Hazards*, **2**, 27-30.
- Boon, J.D., Berquist, J.C.R., (1991). "Evaluation of sediment dynamics and the mobility of heavy minerals on a linear sand shoal". *Journal of Coastal Research*, **7**, 989-1002.
- Chick, L.M.; de Lange, W.P., Healy, T.R., (2001a). "Potential tsunami hazard associated with the Kerepehi Fault, Firth of Thames, New Zealand". *Natural Hazards*, **24**, 309-318.
- Chick, L.M.; Healy, T.R., de Lange, W.P., (2001b). "Tsunami hazard in the Firth of Thames, Hauraki Gulf, New Zealand". *Journal of Coastal Research*, Special Issue **34**, 403-413.
- Chubarov, L.B., Gusiakov, V.K., (1985). "Tsunamis and earthquake mechanisms in the island-arc regions". *Science of Tsunami Hazards*, **3**, 3-21.
- de Lange, W.P., (2000). "The last wave - tsunami". In: Hicks, G., Campbell, H., (eds.), *Awesome forces: the natural hazards that threaten New Zealand*, 2nd ed., Vol. Wellington: Te Papa Press. pp. 98-123.
- de Lange, W.P., Healy, T.R., (1986). "New Zealand tsunamis 1840-1982". *New Zealand Journal of Geology and Geophysics*, **29**, 115-134.
- de Lange, W.P., Healy, T.R., (1997). "Numerical modeling of tsunamis associated with marl diapirism off Poverty Bay, New Zealand". *Proceedings of Combined Australasian Coastal Engineering and Ports Conference, Christchurch*, Vol 1043-1047.
- Downes, G.; Webb, T.; McSaveney, M.; Darby, D.; Doser, D.; Chagué-Goff, C., Barnett, A., (2001a). "The 26 March and 17 May 1947 Gisborne earthquakes and tsunami: implications for tsunami hazard for the east coast, North Island, New Zealand". *Proceedings of International Tsunami Workshop "Tsunami Risk Assessment Beyond 2000: Theory, Practice and Plans"*, Moscow, Russia.
- Downes, G.; Webb, T.; McSaveney, M.; Darby, D.; Doser, D.; Chagué-Goff, C., Barnett, A., (2001b). "The 1947 Gisborne, New Zealand, earthquakes and tsunami". *Proceedings of European Geophysical Society, XXVI General Assembly, Nice, France*, European Geophysical Society.
- Dowrick, D.J., Rhoades, D.A., (1998). "Magnitudes of New Zealand Earthquakes, 1901-1993". *Bulletin Of The New Zealand National Society For Earthquake Engineering*, **31**, 260-280.
- Eiby, G.A., (1982a). "Earthquakes and tsunamis in a region of diapiric folding". *Tectonophysics*, **85**, T1-T8.
- Eiby, G.A., (1982b). "Two New Zealand tsunamis". *Journal Of The Royal Society Of New Zealand*, **12**, 337-351.
- Geist, E.L., (1998). "Local tsunamis and earthquake source parameters". *Advances in Geophysics*, **39**, 117-209.
- Geist, E.L., Dmowska, R., (1999). "Local tsunamis and distributed slip at the source". *Pure and Applied Geophysics*, **154**, 485-512.
- Goldsmith, P.; Barnett, A.; Goff, J.; McSaveney, M.; Elliott, S., Nongkas, M., (1999). "Report of the New Zealand Reconnaissance Team to the area of the 17th July 1998 Tsunami at Sissano Lagoon, Papua New Guinea". *Bulletin of the New Zealand Society for Earthquake Engineering*, **32**, 102-118.
- Grapes, R., Downes, G., (1997). "The 1855 Wairarapa, New Zealand, Earthquake - analysis of historical data". *Bulletin of the New Zealand National Society for Earthquake Engineering*, **30**, 271-368.
- Gusiakov, V.K., (2001). "Red", "Green" and "Blue" tsunamigenic earthquakes and their relation with conditions of oceanic sedimentation in the Pacific. In: Hebenstreit, G.T., (ed.), *Tsunami research at the end of a critical decade*, 18. Dordrecht: Kluwer Academic Publishers. pp. 17-32.
- Hammack, J.L., (1973). "A note on tsunamis: their generation and propagation in an ocean of uniform depth". *Journal of Fluid Mechanics*, **60**, 769-799.
- Hancox, G.T.; Perrin, N.D., Dellow, G.D., (2002). "Recent studies of historical earthquake-induced landsliding, ground damage, and MM intensity in New Zealand". *Bulletin Of The New Zealand National Society For Earthquake Engineering*, **35**, 59-95.
- Hicks, D.M.; Shankar, U., McKerchar, A., (2003). "Sediment yield estimates: a GIS tool". *Water & Atmosphere*, **11**, 26-27.
- Iwasaki, S.I., (1997). "The wave forms and directivity of a tsunami generated by an earthquake and a landslide". *The Science of Tsunami Hazards*, **15**, 23-40.

- Kanamori, H., (1972). "Mechanism of tsunami earthquakes". *Physics of the Earth and Planetary Interiors*, **6**, 346-359.
- Lamarche, G.; Collot, J.-Y.; Garlick, R., de Lange, W.P., (2002). "Submarine avalanche volume calculations, a prerequisite to tsunami modeling: the example of the Ruatoria Debris Avalanche". *Proceedings of European Geophysical Society, XXVII General Assembly, Nice, France*, European Geophysical Society, Vol 4. A150.
- Lewis, K.B.; Garlick, R.; Hill, P.; McKay, K.; Mitchell, J.; Orpin, A., Saunders, H., (2001). "Underwater landscape evolution with NIWA's new MultiBeam". *Water and Atmosphere*, **9**, 24-25.
- Magill, C.R., (2001). "Numerical modelling of tsunami generated by mass movement". MSc thesis, University of Waikato, 198.
- McAdoo, B.G., Watts, P., (2004). "Tsunami hazard from submarine landslides on the Oregon continental slope". *Marine Geology*, **203**, 235-245.
- Pelinovsky, E., Poplavsky, A., (1997). "Simplified model of tsunami generation by submarine landslides". *Physics and Chemistry of the Earth*, **21**, 13-17.
- Reyners, M.; McGinty, P.; Cos, S.; Turnbull, I.; O'Neill, T.; Gledhill, K.; Hancox, G.T.; Beavan, J.; Matheson, D.; McVerry, G.H.; Cousins, J.; Zhao, J.; Cowan, H.; Caldwell, G.; Bennie, S., GeoNet Team, (2003). "The  $M_w$  7.2 Fiordland Earthquake of August 21, 2003: Background and preliminary results". *Bulletin Of The New Zealand National Society For Earthquake Engineering*, **36**, 233-248.
- Ruff, L.J., (2003). "Some aspects of energy balance and tsunami generation by earthquakes and landslides". *Pure and Applied Geophysics*, **160**, 2155-2176.
- Satake, K., Tanioka, Y., (1999). "Sources of tsunami and tsunamigenic earthquakes in subduction zones". *Pure and Applied Geophysics*, **154**, 467-483.
- Stirling, M.W.; McVerry, G.H., Berryman, K.R., (2002). "A new seismic hazard model for New Zealand". *Bulletin of the Seismological Society of America*, **92**, 1878-1903.
- Walters, R.A., (2002). "Long wave resonance on the New Zealand coast". *NIWA*, Technical Report 109, 32 p.
- Ward, S.N., (1980). "Relationships of tsunami generation and an earthquake source". *Journal of Physics of the Earth*, **28**, 441-474.
- Watts, P.; Grilli, S.T.; Kirby, J.T.; Fryer, G.J., Tappin, D.R., (2003). "Landslide tsunami case studies using a Boussinesq model and a fully non-linear tsunami generation model". *Natural Hazards and Earth System Sciences*, **3**, 391-402.
- White-Parsons, G.D., (1944). "The construction of jetties in exposed roadsteads, with particular reference to the reinforced concrete structure provided at Tolaga Bay, New Zealand". *Journal of the Institution of Civil Engineers*, **4**, 214-227.